

Biexciton emission from ZnO/Zn_{0.74}Mg_{0.26}O multiquantum wells

H. D. Sun,^{a)} T. Makino, and Y. Segawa

Photodynamics Research Center, Institute of Physical and Chemical Research (RIKEN), 519-1399 Aoba, Aramaki, Sendai 980-0845, Japan

M. Kawasaki, A. Ohtomo, and K. Tamura

Department of Innovative and Engineered Materials, Tokyo Institute of Technology, Yokohama 226-8502, Japan

H. Koinuma^{b)}

Materials and Structures Laboratory, Tokyo Institute of Technology, Yokohama 226-8503, Japan

(Received 21 February 2001; accepted for publication 3 April 2001)

Luminescence due to the radiative recombination of localized biexcitons has been observed at low temperature (5 K) in ZnO/Zn_{0.74}Mg_{0.26}O multiquantum wells grown by laser-molecular-beam epitaxy on a lattice-matched ScAlMgO₄ substrate (0001). The emission components due to the recombination of localized excitons and biexcitons and due to the exciton–exciton scattering were verified by examining their relative energy positions and intensity dependence on excitation power density. The excitation threshold for biexciton emission was significantly lower than that for exciton–exciton scattering. The binding energy of biexcitons in multi-quantum wells is largely enhanced by quantum confinement effect. © 2001 American Institute of Physics.
[DOI: 10.1063/1.1375830]

Wide band gap semiconductors have been paid intensive attentions for a long time because of their potential applications to meet the commercial need for short wavelength optoelectronic devices. Initially, main efforts were concentrated on ZnSe-based II–VI compound semiconductors.¹ Recently, however, GaN-based materials have progressed more rapidly since the demonstration of blue/green light emitting diodes and laser diodes from InGaN quantum well structures.² Meanwhile, another wide band gap material, ZnO, has also received particular attentions.^{3,4} Compared with III–V nitride materials and other II–VI compound semiconductors, ZnO has larger exciton binding energy (about 60 meV), which in principle should allow for efficient excitonic lasing mechanisms operating at room or even higher temperatures.

Recent experiments have shown that low-threshold stimulated emission or laser action could be achieved in ZnO thin films and ZnO/(Zn, Mg)O multiquantum wells up to room temperature due to inelastic exciton-exciton scattering.^{3–5} It is well established that, at dense excitation, two excitons with opposite spins may interact and form a bound state known as biexciton (or exciton molecules). Biexcitons can play an important role in optical properties such as lower threshold density for stimulated emission or laser action and higher gain coefficient.^{6,7} Such effects related to biexcitons have been observed in a large variety of semiconductors, especially in II–VI wide band gap semiconductors because of their larger binding energy of excitons and biexcitons so that excitons (biexcitons) exist stable at higher density.^{7–14} Luminescence of biexciton recombination has been also reported previously in bulk ZnO,¹⁵ and recently, in ZnO epitaxial layers.¹⁶ It is predicted that this nonlinear optical phenomenon should be more pronounced in low-

dimensional structures like quantum wells because of the enhancement in binding energies of both excitons and biexcitons due to the quantum confinement effect. In this letter, we report on the first observation of luminescence induced by the radiative recombination of localized biexcitons (XX) in high quality ZnO/Zn_{0.74}Mg_{0.26}O multiquantum wells (MQWs) at 5 K. The biexcitonic emission appears at excitation intensity lower than that of emission induced by exciton–exciton scattering. The binding energies of biexcitons in MQWs are largely enhanced compared with that of bulk ZnO.

The ZnO/ZnMgO MQWs were grown on a ScAlMgO₄ substrate (0001) by laser-molecular-beam epitaxy method. The detailed preparation process has been described elsewhere.¹⁷ The total structures consist of 10 periods of alternating ZnO well layers and 5-nm-thick Zn_{1–x}Mg_xO barrier layers. The Mg content of the barrier layers was chosen at $x=0.26$, corresponding to a barrier height of about 0.5 eV. Two samples investigated in this letter have well widths of 3.7 and 1.75 nm, respectively

In Fig. 1, the lowest traces show the photoluminescence (PL, solid line) and optical absorption (dotted line) spectra taken at 5 K from a MQWs sample with well width of 3.7 nm. The PL spectrum is observed in a conventional back-scattering geometry using the 325 nm line of a continuous-wave He–Cd laser as the excitation source. It is dominated by the radiative recombination of localized excitons with peak energy of 3.369 eV and linewidth of about 22 meV, respectively. The lower emission peak at 3.296 eV originates from the 1 LO phonon replica of localized excitonic emission. The difference in peak energies between the PL and excitonic absorption spectra is about 30 meV. This energy difference results from the localization of excitons induced by the fluctuation of well width.

The upper traces [(b), (c), and (d)] in Fig. 1 show the normalized luminescence spectra at various power densities

^{a)}Author to whom correspondence should be addressed; electronic mail: sunhd@postman.riken.go.jp

^{b)}Also a member of CREST, Japan Science and Technology Corporation.

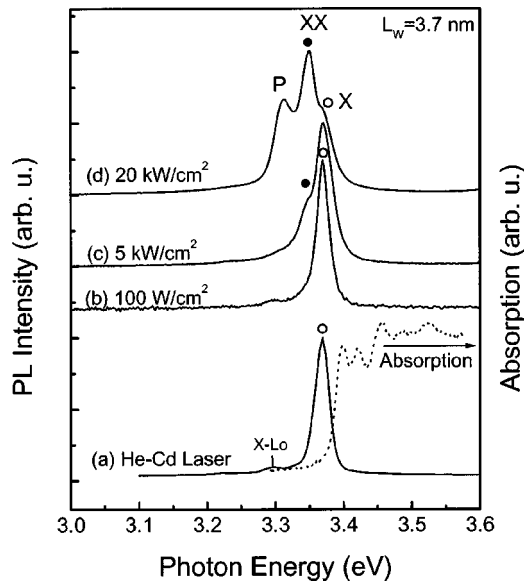


FIG. 1. Luminescence spectra at 5 K taken from a ZnO/Zn_{0.74}Mg_{0.26}O MQW with well width of 3.7 nm under various excitation power densities. The curves have been normalized and relatively shifted. The lowest traces represent the low excitation PL [(a), solid line] and absorption (dotted line) spectra at 5 K for the same sample.

of excitation, taken at 5 K from the same MQW sample. In this case, the optical excitation was carried out by a pulsed dye laser (341 nm) which is pumped by a XeCl excimer laser (308 nm) with a pulse width of ~ 13 ns and a repetition rate of 10 Hz. At the lowest power density [100 W/cm², Fig. 1(b)], the luminescence spectrum is dominated by radiative recombination of localized excitons marked as an open dot (denoted by X), same as low-excitation PL. As the excitation power density increases, there appears a shoulder marked as a solid dot (denoted by XX) on the low-energy side of the X band. This emission band, located at 3.35 eV, grows superlinearly with respect to the excitation intensity. With further increase in excitation intensity, a second peak denoted by P appears at around 3.12 eV. According to the assignment done by the previous studies, the P band originates from inelastic exciton-exciton scattering.⁵

On the basis of the relative energy position, we tentatively assign this newly observed XX band as the radiative recombination of localized biexcitons. This assignment is supported by the dependence of luminescence intensity I_{XX} and I_X on excitation density.

Following Ref. 18, we analyze the excitation power density dependence of luminescence intensity from X and XX in some detail. A system of excitons and biexcitons with densities n_X and n_{XX} can be described by the rate equations,

$$\frac{dn_X}{dt} = G - \frac{n_X}{\tau_X} + \frac{n_{XX}}{\tau_{XX}} - 2 \frac{n_X^2}{n^*} \frac{1}{\tau_C} + 2 \frac{n_{XX}}{\tau_C}, \quad (1a)$$

$$\frac{dn_{XX}}{dt} = -\frac{n_{XX}}{\tau_{XX}} + \frac{n_X^2}{n^*} \frac{1}{\tau_C} - \frac{n_{XX}}{\tau_C}, \quad (1b)$$

where G is the generation rate (proportional to pump power), τ_X and τ_{XX} are the exciton and biexciton lifetimes, and τ_C is the characteristic interconversion time when $n_X = n_{XX} = n^*$. Supposing that exciton emission intensity I_X (biexciton emission intensity I_{XX}) is proportional to n_X (n_{XX}), the re-

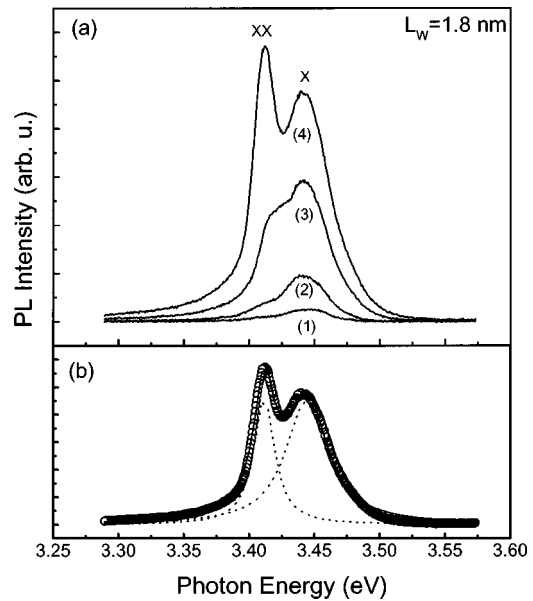


FIG. 2. (a) Luminescence spectra at 5 K taken from a ZnO/Zn_{0.74}Mg_{0.26}O MQW with well width of 1.75 nm under excitation power densities: (1) 248 W/cm², (2) 1257 W/cm², (3) 3347 W/cm², (4) 6417 W/cm², (b) spectral separation procedure of the exciton and biexciton components.

lations between I_X (I_{XX}) and the excitation density can be described by the similar relations. In our experiment, the excitation laser has pulse duration of 13 ns, which is considered to be much longer than the lifetimes of excitons and biexcitons. Therefore, a steady-state condition is established, and the steady-state solutions for I_X (I_{XX}) can be described as¹⁸

$$I_X \propto \left[\left(1 + \frac{G}{G_0} \right)^{1/2} - 1 \right], \quad (2a)$$

$$I_{XX} \propto \left[\left(1 + \frac{G}{G_0} \right)^{1/2} - 1 \right]^2, \quad (2b)$$

where $G_0 = (n^* \tau_{XX} / 4 \tau_X^2) (1 + \tau_C / \tau_X)$ is the characteristic generation rate that separates the exciton-dominant from the biexciton-dominant region. These equations predict that I_X (I_{XX}) grows sublinearly (superlinearly) with the increase in excitation intensity and the exponential factors for I_X and I_{XX} are excitation intensity dependent. However, the relation $I_{XX} \propto I_X^2$ holds true for the whole excitation intensity range where only X and XX contribute to the luminescence spectrum. In practical samples, various emission mechanisms (localized excitons and biexcitons, exciton-phonon and exciton-exciton scattering, plasma, etc.) compete with each other.⁷ As shown in Fig. 1, at high excitation intensity, both the emission from biexciton recombination and emission induced by exciton-exciton scattering appeared in the PL spectrum. However, the former process has much lower excitation threshold than the latter one.

Figure 2(a) shows the PL spectra of another MQWs sample with well width of 1.75 nm at different excitation power densities. In this sample, the biexciton emission emerged at a much lower excitation intensity compared with that shown in Fig. 1. In a range of excitation intensity (0–30 kW/cm²), only two peaks represented by X and XX appeared in the spectra. At higher excitation density the P-band ap-

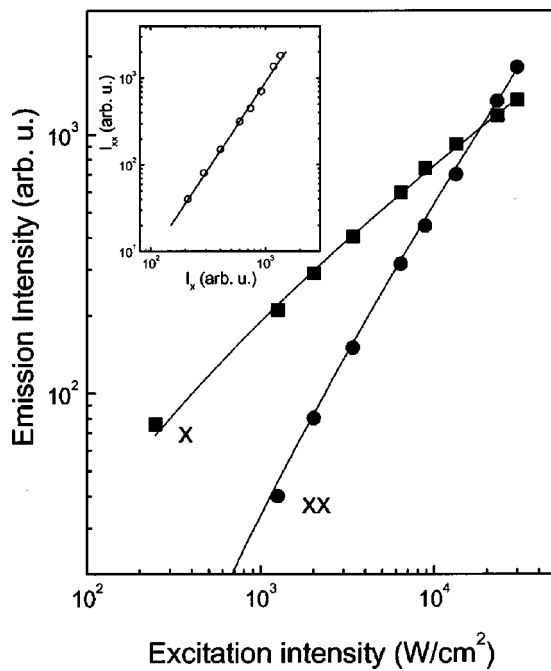


FIG. 3. Exciton and biexciton spectral weights at a temperature of 5 K as functions of excitation power densities for a ZnO/Zn_{0.74}Mg_{0.26}O MQWs sample with well width of 1.75 nm. The solid lines are the fits by using Eq. 2. The inset plots the spectrally integrated intensity I_{XX} as a function of I_X . The solid line denotes the square-power law relation.

appears, same feature as in Fig. 1. We expect that, in this excitation range, only recombinations of localized excitons and biexcitons contribute to the photoluminescence. For quantitative analysis, it is necessary to spectrally separate the exciton and biexciton components in the PL spectra. It is predicted theoretically that the line shape of free biexciton luminescence obeys an inverse Boltzmann or modified distribution.^{19,20} In practical samples, the line shape of biexcitonic luminescence will be complicated by the localization effect because there are distributions of both the localized exciton energy position and the biexciton binding energies.¹¹ Following the procedure described in Ref. 18, the exciton component line shape is determined from a spectrum taken at a low excitation density and scaled as the exciton component in a spectrum for a high excitation density, and the biexciton component I_{XX} is then fit to a Lorentzian line shape while the I_X is adjusted,¹⁸ as illustrated in Fig. 2(b).

In Fig. 3, the solid dots represent the experimental results, and the solid lines represent the calculated results according to Eq. (2). The calculated curves agreed well with the experimental data. In the inset of Fig. 3, we show the biexciton emission intensity I_{XX} as a function of exciton emission intensity I_X . The solid line denotes the square-power law relation. The dependence of I_{XX} on I_X is in close agreement with the square-power law. This gives strong evidence for our assignment.

For the investigated samples, the average biexciton binding energies were determined from the energy separation of the two peaks X and XX to be 19 and 28 meV for MQWs with well widths of 3.7 and 1.75 nm, respectively. For comparison, the biexciton binding energy in bulk ZnO is about 15 meV.¹⁶ Since the well widths of our samples are comparable or smaller than the exciton diameter of ZnO (3.6 nm), the enhancement of biexcitonic binding energies in MQWs

can be reasonably understood to be a consequence of quantum confinement effect in the well growth direction. We believe that the biexciton binding energy in quantum wells could be further enhanced due to the very large exciton binding energy in ZnO.¹¹ In view of the thermal activation energy at $T = 300$ K (~ 25 meV), it is expected that the biexcitonic effect in ZnO-based quantum structures can play an important role at higher temperatures or even room temperature, which is desirable for the realization of ultralow threshold lasers.

In summary, we have studied the dependence of exciton-related luminescence on excitation intensity in ZnO/Zn_{0.74}Mg_{0.26}O MQWs. We observed the luminescence due to the radiative recombination of localized biexcitons at low temperature in ZnO-based quantum well structures. The biexciton emission emerged at much lower excitation intensity than that of exciton-exciton scattering. The biexciton binding energy in MQWs was largely enhanced compared with bulk ZnO due to the quantum confinement effect.

This work was supported by the Proposal Based Program of NEDO and partially by the Special Postdoctoral Research Program of RIKEN, Japan.

- ¹H. Jeon, J. Ding, A. V. Nurmikko, H. Luo, N. Samarth, J. K. Furdyna, W. A. Bonner, and R. E. Nahory, *Appl. Phys. Lett.* **57**, 2413 (1990).
- ²S. Nakamura, M. Senoh, S. Nakahana, N. Iwasa, T. Yamada, T. Matsushita, Y. Sugimoto, and H. Kiyoku, *Appl. Phys. Lett.* **69**, 1477 (1996).
- ³P. Yu, Z. K. Tang, G. K. L. Wong, M. Kawasaki, A. Ohtomo, H. Koinuma, and Y. Segawa, *Solid State Commun.* **103**, 459 (1997); Y. Segawa, A. Ohtomo, M. Kawasaki, H. Koinuma, Z. K. Tang, P. Yu, and G. K. L. Wong, *Phys. Status Solidi B* **202**, 669 (1997); Z. K. Tang, G. K. L. Wong, P. Yu, M. Kawasaki, A. Ohtomo, H. Koinuma, and Y. Segawa, *Appl. Phys. Lett.* **72**, 3270 (1998).
- ⁴D. M. Bagnall, Y. Chen, Z. Zhu, T. Yao, S. Koyama, M. Y. Shen, and T. Goto, *Appl. Phys. Lett.* **70**, 2230 (1997).
- ⁵A. Ohtomo, K. Tamura, M. Kawasaki, T. Makino, Y. Segawa, Z. K. Tang, G. K. L. Wong, Y. Matsumoto, H. Koinuma, *Appl. Phys. Lett.* **77**, 2204 (2000). H. D. Sun, T. Makino, N. T. Tuan, Y. Segawa, Z. K. Tang, G. K. L. Wong, M. Kawasaki, A. Ohtomo, and K. Tamura, and H. Koinuma, *Appl. Phys. Lett.* **77**, 4250 (2000).
- ⁶M. Sugawara, *Jpn. J. Appl. Phys., Part 1* **35**, 124 (1996).
- ⁷F. Kreller, M. Lowisch, J. Puls, and F. Henneberger, *Phys. Rev. Lett.* **75**, 2420 (1995); F. Kreller, J. Puls, and F. Henneberger, *Appl. Phys. Lett.* **69**, 2406 (1996).
- ⁸C. Klingshirn and H. Haug, *Phys. Rep.* **70**, 315 (1981).
- ⁹E. Hanamura and H. Haug, *Phys. Rep.* **33**, 209 (1977).
- ¹⁰S. Charbonneau, T. Steiner, M. L. W. Thewalt, E. S. Koteles, J. Y. Chi, and B. Elman, *Phys. Rev. B* **38**, 3583 (1988).
- ¹¹F. Gindele, U. Woggon, W. Langbein, J. M. Hvam, K. Leonardi, D. Hommel, and H. Selke, *Phys. Rev. B* **60**, 8773 (1999); W. Langbein, J. M. Hvam, M. Umlauff, H. Kalt, B. Jobst and D. Hommel, *ibid.* **55**, R7383 (1997).
- ¹²Y. Yamada, T. Sakashita, H. Watanabe, H. Kugimiya, S. Nakamura, and T. Taguchi, *Phys. Rev. B* **61**, 8363 (2000).
- ¹³Y. F. Wei, D. M. Huang, X. J. Wang, G. C. Yu, C. S. Zhu, and X. Wang, *Appl. Phys. Lett.* **74**, 1138 (1999).
- ¹⁴V. Kozlov, P. Kelkar, A. V. Nurmikko, C. C. Chu, D. C. Grillo, J. Han, C. G. Hua, and R. L. Gunshor, *Phys. Rev. B* **53**, 10837 (1996).
- ¹⁵J. M. Hvam, G. Blattner, M. Reuscher, and C. Klingshirn, *Phys. Status Solidi B* **118**, 179 (1983).
- ¹⁶H. J. Ko, Y. F. Chen, T. Yao, K. Miyajima, A. Yamamoto, and T. Goto, *Appl. Phys. Lett.* **77**, 537 (2000).
- ¹⁷Y. Matsumoto, M. Murakami, Z. W. Jin, A. Ohtomo, M. Lippmaa, M. Kawasaki, and H. Koinuma, *Jpn. J. Appl. Phys., Part 2* **38**, L603 (1999).
- ¹⁸J. C. Kim, D. R. Wake, and J. P. Wolfe, *Phys. Rev. B* **50**, 15099 (1994).
- ¹⁹H. Souma, T. Goto, T. Ohta, and M. Ueta, *J. Phys. Soc. Jpn.* **29**, 697 (1970).
- ²⁰G. Kuang, W. Gebhardt, E. Griehl, K. Sube, M. Kastner, M. Wörz, and T. Reisinger, *Appl. Phys. Lett.* **70**, 2717 (1997).